An Efficient Calculational Approach to Evaluation of Microwave Specific Attenuation

Le-Wei Li, *Senior Member, IEEE*, Tat-Soon Yeo, *Senior Member, IEEE*, Pang-Shyan Kooi, *Member, IEEE*, and Mook-Seng Leong, *Senior Member, IEEE*

***Abstract*—An efficient calculational approach using the scattering-radiation conversion is developed in this paper to evaluate the microwave attenuation by arbitrarily distorted raindrops. For this modified first-order approach, the perturbation technique and the spherical vector eigenfunction expansion method are employed. A method of obtaining the volumetric current distribution of the assumed source that generates the plane waves is developed in the paper and the current distribution of such a source is derived. The electromagnetic fields outside the distorted raindrop scatterers are formulated in terms of integrals consisting of a volumetric current distribution located at infinity and the dyadic Green's functions. To illustrate the validity of this approach, the spheroidal raindrop and the Pruppacher and Pitter (P–P) raindrop model of varying shapes are specifically investigated. Numerical results of the extinction cross sections and the specific attenuation due to the two models are obtained. While the former agrees well with the published results, the latter is in good agreement with the experimental specific attenuation data collected at 21.225 GHz in Singapore.**

***Index Terms*—Microwave propagation effects, rain.**

I. Introduction

To investigate the scattering of plane electromagnetic waves by distorted raindrop scatterers, many methods have been developed since the 1970s. The methods that received most attention over the past 30 years are: *Rayleigh–Debye* (R–D) approximation (or the Born approximation) [1], [2], the perturbation theory proposed by Oguchi [3], [4] and utilized by Li *et al.* [5], [6], the least squares fitting technique developed by Morrison and Cross [7], [8], the T-matrix method originated by Waterman [9], [10], the extended boundary condition method described by Barber and Yeh [11] and by Warner and Hizal [12], the unimoment method given by Mei and Chang [13], [14], and some others introduced in Oguchi's reviews [15], [16]. Although each of them has its own shortcomings, nevertheless, they have made significant contributions to the problem of microwave attenuation due to rainfall.

In order to investigate the attenuation of plane electromagnetic waves due to rainfall, one first assumes certain physical models for the raindrop shapes and then obtains the total or extinction cross sections (TCSs) of the raindrop scatterers. The simplest and the most typical raindrop model used in the evaluation of the microwave rainfall attenuation is the sphere [17] and the simplest technique is the Mie's scattering theory. However, the spherical model of raindrop shapes is only valid for very small raindrops [16], as shown in the photographic measurements of raindrop shapes [18], [19]. As the raindrop becomes larger, the oblate spheroidal model can be used to describe the shapes of the raindrops well. To improve the evaluation of the attenuation by raindrops, modification of the raindrop model from sphere to spheroid was made to investigate the effects of distortions of the raindrop shapes. However, as the raindrop becomes fairly large, the shapes of the raindrops are greatly distorted, and no longer spheroids [16], [20]. Their shapes look like a Hamburger and are nonaxisymmetric. Theoretically, Pruppacher and Pitter (P–P) [21] established an equation to describe the shapes of water drops falling at their terminal velocity in terms of the balance of the internal and external pressures on the surfaces of the drops. This model of varying shapes has been well accepted by researchers in the calculation of microwave specific attenuation [16], [12], [15]. According to the P–P raindrop model, the raindrop looks like a sphere, as its size is very small, then a spheroid or ellipsoid as the size increases, and finally a Hamburger-shaped scatterer as the size becomes fairly large.

To show these effects, Oguchi solved the P–P equation numerically and evaluated 13 raindrop shapes [16] for the different drop sizes used first by Laws and Parsons in their drop-size distribution [22]. However, the P–P equation is almost impossible to be solved analytically so that further approximation is needed to simplify the scattering problem for practical engineering applications. In order to include the effects of large-scale distortion of raindrops on the microwave attenuation Oguchi [16] utilized the cosine series to simulate the varying shapes of the raindrops. However, the cosine series in turn introduces further complication to the mathematical expressions of the scattered fields and the TCS so that a numerical technique has to be employed at the beginning of the evaluation [23]. Hence, considerable amount of computer time is needed for the computation. The amount of computer time may be reduced using a simple expression of the raindrop shapes by Li *et al.* [20].

This paper aims at solving for the scattered field due to an arbitrarily shaped raindrops by means of an efficient and simple integral equation approximation developed based on the scattering-radiation conversion. It is well known that the key problem in making use of integral equation method to derive the scattered electromagnetic fields outside the scatterers is the representation of the transmitted electromagnetic fields inside the scatterers. Rayleigh approximation, as a representative

Manuscript received October 5, 1998; revised March 4, 1999. This work was supported in part by a grant under the NUS/Telecoms Joint R&D Project 018 and an ARF Grant under the RP 981619.

The authors are with Communications and Microwave Division, Department of Electrical Engineering, National University of Singapore, Singapore 119260 (e-mail: LWLi@nus.edu.sg).

Publisher Item Identifier S 0018-926X(00)06938-6.

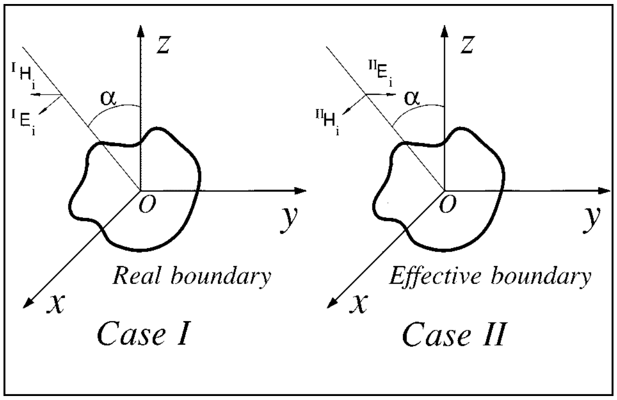

Fig. 1. Scattering of the plane waves polarized horizontally (II) and vertically (I) by an arbitrarily shaped scatterer.

example, replaces the transmitted wave inside the scatterers by the incident plane wave to enable the scattered fields outside the scatterers to be integrated and expressed analytically. To improve the calculation, the Rytov approximation [24] is developed. The Rytov approximation shares some similarity with the WKB approximation [24] and is, therefore, a weak scattering approximation even if it works better at higher frequencies than the Rayleigh–Debye (R–D) approximation. The Fredholm integral equation method and the T-matrix method use the integral operators to expand the scattered electromagnetic fields into an infinite series, with each term in the series representing an integral corresponding to the different-order approximation. It is, however, almost impossible to integrate analytically each of the infinite series in practical engineering problems, so that a further approximation has to be made.

II. Statement of the Problem

Consider the geometry shown in Fig. 1 where an incident plane electromagnetic wave is scattered by a homogeneous but arbitrarily shaped raindrop. The incident waves have vertical (I corresponding to the y-directed magnetic field) and horizontal (II corresponding to the y-directed electric field) polarizations, as illustrated in Fig. 1. A source generating the plane waves is assumed to be located at infinity.

The total electric field $\boldsymbol{E}$ of an electromagnetic wave everywhere is governed by the Maxwell's equations. The wave equations can be expressed as follows [25] if suppressing the time factor $e^{i\omega t}$:

$$\nabla \times \nabla \times \boldsymbol{E}(\boldsymbol{r}) - k^2\boldsymbol{E}(\boldsymbol{r}) = -i\omega\mu\boldsymbol{J}(\boldsymbol{r}')\delta(\boldsymbol{r}-\boldsymbol{r}') \qquad (1)$$

where $k^2 = \omega\mu(\omega\epsilon - i\sigma)$, and μ, ϵ and σ are the permeability, the permittivity, and the conductivity, respectively. In free-space, we have $k_0^2 = \omega^2\epsilon_0\mu_0$.

The solution to (1) may be represented in terms of the integral including the electric type of dyadic Green's function as follows:

$$\boldsymbol{E}(\boldsymbol{r}) = -i\omega\mu \iiint_V \overline{\boldsymbol{G}}_e(\boldsymbol{r}, \boldsymbol{r}') \cdot \boldsymbol{J}(\boldsymbol{r}')\, d\boldsymbol{r}' \qquad (2)$$

where the Green's dyadic $\overline{\boldsymbol{G}}_e(\boldsymbol{r}, r')$ is given in Appendix A and the electric volumetric current distribution $\boldsymbol{J}(\boldsymbol{r}')$ is formulated in Appendix B using the eigenfunction expansion of the incident field and the unbounded Green's dyadic.

Comparing with the scattering coefficients of the plane wave obtained from the Mie theory for a spherical scatterer, we find that $\mathcal{S}_n^a(a_e)$ and $\mathcal{S}_n^b(a_e)$ of the dyadics derived in Appendix A are similar to those scattering coefficients of the Mie theory. In the above consideration, the arbitrarily shaped scatterer was treated as an equivalent sphere so as to simplify our derivation.

Thus, the electric field outside an equivalent sphere shown in (2) for different polarizations I and II can be rewritten as

$$\begin{aligned} {}^{I}_{II}\boldsymbol{E}(\boldsymbol{r}) &= i\omega\mu \iiint_V \overline{\boldsymbol{G}}_{e0}(\boldsymbol{r}, \boldsymbol{r}') \cdot {}^{I}_{II}\boldsymbol{J}(\boldsymbol{r}')\, d\boldsymbol{r}' \\ &\quad + i\omega\mu \iiint_V \overline{\boldsymbol{G}}_{es}(\boldsymbol{r}, \boldsymbol{r}') \cdot {}^{I}_{II}\boldsymbol{J}(\boldsymbol{r}')\, d\boldsymbol{r}' \\ &= {}^{I}_{II}\boldsymbol{E}_i(\boldsymbol{r}) + \iiint_V \overline{\boldsymbol{G}}_{es}(\boldsymbol{r}, \boldsymbol{r}') \cdot {}^{I}_{II}\boldsymbol{J}(\boldsymbol{r}')\, d\boldsymbol{r}' \end{aligned} \qquad (3)$$

where the subscript of the integral V denotes the volume of the raindrop scatterer. The first term of (3) represents the direct waves due to the source ${}^{I}_{II}\boldsymbol{J}(\boldsymbol{r}')$. In this problem shown in Fig. 1, it is just the incident waves of respective polarizations. The second term, on the other hand, is the scattered field.

The incident fields have been given by Morrison and Cross in [8]. Using the orthogonal properties of $\boldsymbol{M}_{\substack{e\\o}mn}(k_0)$ and $\boldsymbol{N}_{\substack{e\\o}mn}(k_0)$, the incident fields can be expanded in a series of vector wave functions [3], [8]. The expanded forms of the electromagnetic incident fields are given by

$${}^{I}_{II}\boldsymbol{E}_i = \sum_{n=1}^{\infty}\sum_{m=0}^{n}\left[{}^{I}_{II}\mathcal{A}^i_{\substack{o\\e}mn}\boldsymbol{M}_{\substack{o\\e}mn} + {}^{I}_{II}\mathcal{B}^i_{\substack{e\\o}mn}\boldsymbol{N}_{\substack{e\\o}mn}\right] \qquad (4a)$$

and

$${}^{I}_{II}\boldsymbol{H}_i = \frac{ik_0}{\omega\mu_0}\sum_{n=1}^{\infty}\sum_{m=0}^{n}\left[{}^{I}_{II}\mathcal{A}^i_{\substack{o\\e}mn}\boldsymbol{N}_{\substack{o\\e}mn} + {}^{I}_{II}\mathcal{B}^i_{\substack{e\\o}mn}\boldsymbol{M}_{\substack{e\\o}mn}\right] \qquad (4b)$$

where the coefficients, ${}^{I}_{II}\mathcal{A}^i_{\substack{o\\e}mn}$ and ${}^{I}_{II}\mathcal{B}^i_{\substack{e\\o}mn}$ are given as follows:

$$\begin{bmatrix} {}^{I}\mathcal{A}^i_{\substack{o\\e}mn} \\ {}^{II}\mathcal{A}^i_{\substack{o\\e}mn} \end{bmatrix} = \frac{(2-\delta_m^0)(2n+1)}{n(n+1)}\,\frac{(n-m)!}{(n+m)!} \cdot (-i)^n \begin{bmatrix} E_I \dfrac{mP_n^m(\cos\alpha)}{\sin\alpha} \\ -E_{II}\dfrac{dP_n^m(\cos\alpha)}{d\alpha} \end{bmatrix} \qquad (5a)$$

and

$$\begin{bmatrix} {}^{I}\mathcal{B}^i_{\substack{e\\o}mn} \\ {}^{II}\mathcal{B}^i_{\substack{e\\o}mn} \end{bmatrix} = -\frac{(2-\delta_m^0)(2n+1)}{n(n+1)}\,\frac{(n-m)!}{(n+m)!} \cdot (-i)^n \begin{bmatrix} E_I \dfrac{dP_n^m(\cos\alpha)}{d\alpha} \\ E_{II}\dfrac{mP_n^m(\cos\alpha)}{\sin\alpha} \end{bmatrix}. \qquad (5b)$$

The total electromagnetic field outside the raindrop should be the sum of the incident (direct-wave) field and the scattered field due to the existence of the raindrops. The first term in (3) represents the contribution due to the direct waves in unbounded space and, therefore, is independent of the raindrop shape. The second term in (3) represents the contribution due to waves scattered by the raindrop surface. Once the current distribution of the source that generates the plane waves has been evaluated, the scattered field due to the raindrop surface can, therefore, be obtained from the second term integral of (3) with the dyadic Green's function for the spheroid as the kernel of integration.

III. Formulation of Scattered Fields

Among the existing methods in deriving the scattered fields, the most well-known are: 1) Rayleigh–Debye (R–D), Rayleigh–Gans, or Born approximations that simply replace the transmitted wave inside the scatterers by the incident plane wave [26] and 2) the modified Rayleigh–Debye approximation which uses a method similar to that of R–D approximation, except it replaces the propagation constant of the incident plane wave outside the scatterer by that inside the scatterer [27], [28].

In this paper, the knowledge of transmitted field inside such an arbitrarily shaped scatterer is not required. The approximation is made to modify the reflection coefficients and vector wave functions. The zeroth-order scattering from the spheroid is, of course, the Mie scattering from a sphere. The first-order scattering approximation can be made by either 1) modifying the reflection coefficients $\mathcal{S}_n^a(a_e)$ and $\mathcal{S}_n^b(a_e)$ using an effective radius for the spheroid or 2) modifying the spherical vector wave functions to the spheroidal functions. Obviously, to modify the reflection coefficients is easier.

A. Scattered Fields from Arbitrarily Shaped Scatterers

Consider an arbitrarily distorted scatterer of which the surface is expressed by the following equation:

$$r = a\left[1 + \nu f(\theta', \phi')\right] \tag{6}$$

where θ' and ϕ' denote the zenith angle and the azimuth angle of the incident waves at which the reflection occurs. If the parameter ν in (6) is small enough, the second term is only a distortion based on a sphere with a radius a. Thus, we can consider $a[1+\nu f(\theta', \phi')]$ as the effective radius a_e of the arbitrarily shaped scatterer.

Using the relation $a[1 + \nu f(\theta', \phi')]$ instead of the effective radius a_e, the scattered field in the analogous expansions can be obtained and represented in terms of the spherical Bessel functions as follows:

$${}^{I}_{II}\boldsymbol{E}_s = \sum_{n=1}^{\infty}\sum_{m=0}^{n}\left[{}^{I}_{II}\mathcal{A}^s_{{}^o_e mn}\boldsymbol{M}^{(2)}_{{}^o_e mn} + {}^{I}_{II}\mathcal{B}^s_{{}^e_o mn}\boldsymbol{N}^{(2)}_{{}^e_o mn}\right] \tag{7a}$$

and

$${}^{I}_{II}\boldsymbol{H}_s = \frac{ik_0}{\omega\mu_0}\sum_{n=1}^{\infty}\sum_{m=0}^{n}\left[{}^{I}_{II}\mathcal{A}^s_{{}^o_e mn}\boldsymbol{N}^{(2)}_{{}^o_e mn} + {}^{I}_{II}\mathcal{B}^s_{{}^e_o mn}\boldsymbol{M}^{(2)}_{{}^e_o mn}\right] \tag{7b}$$

where the coefficients of the electromagnetic fields are given by

$${}^{I}_{II}\mathcal{A}^s_{{}^o_e mn} = \frac{ik_0}{4\pi}\sum_{n'=1}^{\infty}\sum_{m'=0}^{n}(2-\delta_0)\frac{2n+1}{n(n+1)}\frac{(n-m)!}{(n+m)!} \cdot \lim_{r_0\to\infty}\left[\iiint \mathcal{S}_n^a\left(a\left[1+\nu f(\theta', \phi')\right]\right) \cdot \boldsymbol{M}'_{{}^o_e mn}(k) \cdot {}^{I}_{II}\boldsymbol{J}(\boldsymbol{r}')\,d\boldsymbol{r}'\right] \tag{8a}$$

and

$${}^{I}_{II}\mathcal{B}^s_{{}^e_o mn} = \frac{ik_0}{4\pi}\sum_{n'=1}^{\infty}\sum_{m'=0}^{n}(2-\delta_0)\frac{2n+1}{n(n+1)}\frac{(n-m)!}{(n+m)!} \cdot \lim_{r_0\to\infty}\left[\iiint \mathcal{S}_n^b\left(a\left[1+\nu f(\theta', \phi')\right]\right) \cdot \boldsymbol{N}'_{{}^e_o mn}(k) \cdot {}^{I}_{II}\boldsymbol{J}(\boldsymbol{r}')\,d\boldsymbol{r}'\right]. \tag{8b}$$

To integrate (8a) and (8b), (B.5) together with Eq. (B.9) should be used here. To compare our results obtained here with those published elsewhere [3], [8], the Taylor expansion with respect to the perturbation $\nu f(\theta, \phi)$ should be made in (8a) and (8b). However, it is found that a closed form of the above integral can be derived, without any expansion.

The scattering coefficients derived from the integration may be written as

$$\frac{{}^{I}_{II}\mathcal{A}^s_{{}^o_e mn}}{{}^{I}_{II}\mathcal{A}^i_{{}^o_e mn}} = \frac{-j_n(\zeta\rho_{\text{eff}})[\rho_{\text{eff}}j_n(\rho_{\text{eff}})]' + j_n(\rho_{\text{eff}})[\zeta\rho_{\text{eff}}j_n(\zeta\rho_{\text{eff}})]'}{j_n(\zeta\rho_{\text{eff}})[\rho_{\text{eff}}h_n^{(2)}(\rho_{\text{eff}})]' - h_n^{(2)}(\rho_{\text{eff}})[\zeta\rho_{\text{eff}}j_n(\zeta\rho_{\text{eff}})]'} \tag{9a}$$

$$\frac{{}^{I}_{II}\mathcal{B}^s_{{}^e_o mn}}{{}^{I}_{II}\mathcal{B}^i_{{}^e_o mn}} = \frac{-j_n(\rho_{\text{eff}})[\zeta\rho_{\text{eff}}j_n(\zeta\rho_{\text{eff}})]' + \zeta^2 j_n(\zeta\rho_{\text{eff}})[\rho_{\text{eff}}j_n(\rho_{\text{eff}})]'}{h_n^{(2)}(\rho_{\text{eff}})[\zeta\rho_{\text{eff}}j_n(\zeta\rho_{\text{eff}})]' - \zeta^2 j_n(\zeta\rho_{\text{eff}})[\rho_{\text{eff}}h_n^{(2)}(\rho_{\text{eff}})]'} \tag{9b}$$

where $\zeta = \sqrt{\epsilon_r}$ is the relative refractive index given numerically by Ray [31] in his Fortran program and the intermediate ρ_{eff} is defined by

$$\rho_{\text{eff}} = k_0 a_{\text{eff}} = k_0 a\left[1 + \nu f(\alpha, 0)\right] \tag{10}$$

with the effective radius provided later in Table I.

From (9) and (10), we can see that the scattering coefficients ${}^{I}_{II}\mathcal{A}^s_{{}^o_e mn}$ and ${}^{I}_{II}\mathcal{B}^s_{{}^e_o mn}$ can be derived very easily, provided that the shape of the scatterer given by (6) is known.

B. Scattered Fields from Spheroidal Raindrops

As an application of the method developed here, a case where the coefficients of scattered electromagnetic fields are due to spheroidal raindrops is formulated. The applicability of the method presented here will be numerically examined later.

As the raindrop scatterers are spheroidal, the surface of the raindrops may be described as [3], [4], [8], [29], [30]:

$$r = \frac{a}{\sqrt{1-\nu\sin^2\theta}} \approx a\left[1 + \frac{1}{2}\nu\sin^2\theta\right] \tag{11}$$

where $\nu = 1 - (a/b)^2$, and a and b (all in centimeters) are the oblate spheroidal minor and major semiaxes. They can be determined from the mean raindrop radius $\overline{a}$ by two methods developed for the specific microwave attenuation due to rainfall. One was used by Oguchi [3] by assuming that

$$ab^2 = \overline{a}^3 \quad \left(\frac{a}{b}\right)^2 = \nu = 1 - \frac{4.1}{4.5}\overline{a}$$

while the other was given by Morrison and Cross [8] by assuming that

$$ab^2 = \overline{a}^3 \quad \frac{a}{b} = 1 - \overline{a}$$

provided that $\overline{a}$ (in centimeters) is known. In this paper, for spheroidal raindrops, the set of parameters given by Morrison and Cross are adopted to compute the effective raindrop radii.

Following the similar procedure given previously, we find that the scattering coefficients of the electromagnetic fields due to the existence of the spheroidal raindrops are expressed exactly in the same form of (9) except that the intermediate $\rho_{\rm eff}$ in (10) needs to be rewritten as

$$\rho_{\rm eff} = k_0 a_{\rm eff} = \frac{k_0 a}{\sqrt{1 - \nu \sin^2\alpha}} \approx a\left[1 + \frac{1}{2}\nu\sin^2\alpha\right]. \quad (12)$$

The solution that we have obtained, as can be seen, is of a closed form. To compare the results derived here with those published elsewhere, we may expand the formula in (9). Under the first-order approximation, using (12) we derive the scattering coefficients given by

$$\begin{bmatrix} {}^{I}_{II}\mathcal{A}^{s}_{{}^{e}_{o}mn} \\ {}^{I}_{II}\mathcal{B}^{s}_{{}^{e}_{o}mn} \end{bmatrix} \approx \left\{ \begin{bmatrix} \mathcal{S}^a_n \\ \mathcal{S}^b_n \end{bmatrix} + \frac{1}{2}\nu\sin^2\alpha \begin{bmatrix} \dfrac{d\mathcal{S}^a_n(a_{\rm eff})}{da_{\rm eff}} \\ \dfrac{d\mathcal{S}^b_n(a_{\rm eff})}{da_{\rm eff}} \end{bmatrix} \right\} \cdot \begin{bmatrix} {}^{I}_{II}\mathcal{A}^{i}_{{}^{o}_{e}mn} \\ {}^{I}_{II}\mathcal{B}^{i}_{{}^{e}_{o}mn} \end{bmatrix}. \quad (13)$$

Comparing with the scattering coefficients derived by Oguchi [3], Morrison and Cross [8], and Li *et al.* [5], the scattering coefficients presented above in (13) are consistent. The first term given in (13) represents the Mie scattering coefficients due to an equivolumetric sphere of the effective radius $a_{\rm eff}$, while the second term represents the first-order perturbation coefficients due to the distortion based on the sphere. It should be pointed out that the expanded form of the scattering coefficients is used only for the *comparison*. In our formulas of the scattering coefficients, such an expansion is *unnecessary* since it is an extra mathematical approximation and therefore introduces errors due to the negligence of the higher order terms in the Taylor expansion.

C. –Scattered Fields from P–P Model Raindrops

The P–P model raindrops was modified and represented in [20]. This model has been successfully utilized by Li *et al.* [5], [6] in the computation of the specific microwave attenuation using the extended boundary condition and point fitting technique. Under the spherical coordinates system, the model is expressed for $0 \le \phi \le 2\pi$ by

$$r = a(1-\nu_1)\left[f_0(\theta) + \frac{\nu_1}{1-\nu_1}f_1(\theta)\right] = \begin{cases} a(1-\nu_1)\left[1 + \dfrac{\nu_1}{1-\nu_1}\sin^2\theta\right], & 0 \le \theta \le \pi/2 \\ a(1-\nu_2)\left[1 + \dfrac{\nu_2}{1-\nu_2}\sin^2\theta\right], & \pi/2 \le \theta \le \pi \end{cases} \quad (14)$$

where

$$a = 1.111\,582\overline{a} \quad (15a)$$

$$\nu_1 = -1.375\,447 \times 10^{-2} + 6.543\,960 \times 10^{-2}a \quad (15b)$$

$$\nu_2 = -7.239\,211 \times 10^{-2} + 1.827\,561 \times 10^{-1}a \quad (15c)$$

$$f_0(\theta) = 1 - \frac{\nu_2 - \nu_1}{1-\nu_1}H\left(\theta - \frac{\pi}{2}\right) \quad (15d)$$

$$f_1(\theta) = \left[1 + \frac{\nu_2 - \nu_1}{\nu_1}H\left(\theta - \frac{\pi}{2}\right)\right]\sin^2\theta \quad (15e)$$

while $\overline{a}$ denotes the raindrop mean radius introduced by Laws and Parsons [22] and Oguchi [23], and $H(\theta)$ represents the step function.

With this P–P model, the shape of the raindrop is a function of its size. Fig. 2 shows the normalized shapes of the raindrops obtained from the cosine series of the simplified distorted model. The raindrop radius ranges from 0.25 mm in Fig. 2(a) to 3.0 mm in Fig. 2(l) with a step increment of 0.25 mm. It can be seen from the comparison that the shape of the raindrop looks like a sphere for a very small size raindrop, an oblate spheroid for a medium size raindrop, and a hamburger for a fairly large size raindrop.

In our computation, the intermediate effective radius can be expressed by

$$\rho_{\rm eff} = k_0\overline{a}(1-\nu_1)\left[f_0(\alpha) + \frac{\nu_1}{1-\nu_1}f_1(\alpha)\right]. \quad (16)$$

IV. Total (Extinction) Cross Sections

To gain an insight into the characteristics of spheroidal and P–P model raindrops, the TCSs are calculate in this section and compared with those numerical results previously published [3], [5], [8].

The total (or extinction) cross section (TCS) is defined [3], [8] by the ratio of the extinction energy (including absorbed and scattered energies) to the mean energy flow of the incident wave per unit area. For the case under consideration here, the TCS can be expressed as

$$Q_t = -\frac{2\pi}{k_0^2}\Re e\sum_{n=1}^{\infty}(2n+1)[S^a_n(a_{\rm eff}) + S^b_n(a_{\rm eff})] \quad (17)$$

where the scattering coefficients S^a_n and S^b_n have been given by (9) together with (12).

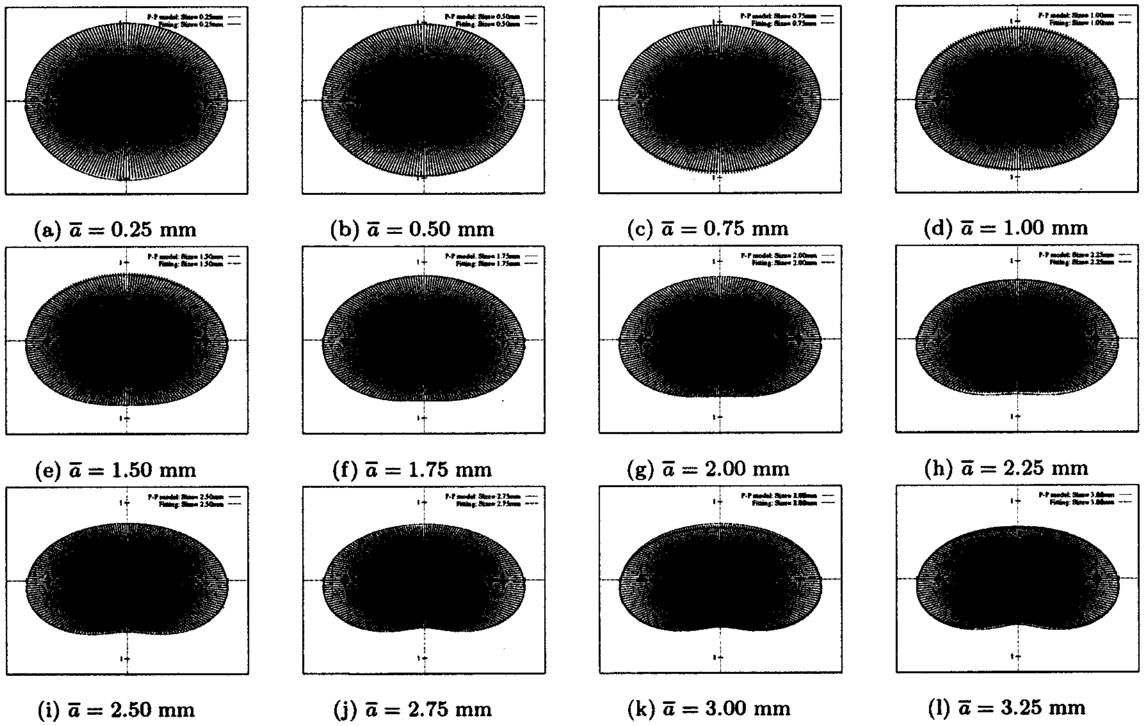

Fig. 2. Normalized raindrop shapes obtained using the cosine series of the simplified P–P model for different sizes.

TABLE I
RAINDROP PARAMETERS AGAINST DROPSIZE FOR DIFFERENT MODELS

Mean raindrop radius	Parameters used by Oguchi [3]		Parameters used by Morrison/Cross [8]		Effective radius utilized in this paper	
					Spheroid	P-P model
$\bar{a}$ (mm)	a (mm)	ν	a (mm)	ν	a_{eff} (mm)	a_{eff} (mm)
0.25	0.246	.0541	0.2458158	0.049375	0.2521	0.250351
0.50	0.485	.0889	0.4831913	0.0975	0.5086	0.502601
0.75	0.715	.1319	0.7120149	0.144375	0.7697	0.760034
1.00	0.938	.1739	0.9321698	0.19	1.0357	1.021387
1.25	1.153	.2148	1.1435330	0.234375	1.3069	1.295390
1.50	1.360	.2547	1.3459757	0.2775	1.5835	1.575728
1.75	1.559	.2934	1.5393617	0.319375	1.8659	1.866811
2.00	1.749	.3312	1.7235477	0.36	2.1544	2.164876
2.25	1.931	.3680	1.8983822	0.399375	2.4495	2.469136
2.50	2.104	.4037	2.0637045	0.4375	2.7516	2.778872
2.75	2.269	.4383	2.2193444	0.474375	3.0612	3.093715
3.00	2.425	.4719	2.3651206	0.51	3.3787	3.413975
3.25	2.572	.5045	2.5008398	0.544375	3.7049	3.742130

Since only the forward scattering is needed for comparison with the measured results, we will consider the polar angle of 90° in this section. To compute the TCS numerically, appropriate raindrop parameters should be chosen. In Table I, the mean raindrop radius $\bar{a}$ of the equivolumetric spherical raindrops are listed. Based on the equivolumetric spheres, two sets of raindrop parameters are obtained by Oguchi [3], and Morrison and Cross [8], respectively. The formulas used to acquire the data listed have been given in the previous section. Since the set of parameters given by Morrison and Cross [8] can be used to obtain reasonably consistent results for the larger drop sizes, it is used in this paper to calculate the effective radii.

A. Spheroidal Raindrops

Numerically, the TCSs of spheroidal raindrops at operating frequencies of 4, 11, 18.1, and 30 GHz are calculated. The relative refractive indexes at the temperature of 20 °C corresponding to the above four frequencies are calculated from Ray's Fortran code [31], which gives (8.7800, $-i0.9777$), (7.8835, $-i2.1848$), (6.8576, $-i2.7169$), and (5.5793, $-i2.8481$), respectively. The numerical results of the TCSs computed here are compared in Fig. 3 with Morrison and Cross's data at frequencies of 4, 11, 18.1, and 30 GHz. In Fig. 3, "*simple*" denotes the TCSs of spheroidal raindrops obtained in this paper using the "*simple*" method developed, and "*fitting*" represents the TCSs for horizontal polarization of the spheroidal raindrops published by Morrison and Cross using the least squares process of the boundary conditions. The TCSs obtained here at each frequency, as can be seen from Fig. 3, are quite close to those TCSs for horizontal polarization given by Morrison and Cross [8], demonstrating the applicability of the simple method.

B. P–P Model Raindrops

Numerical results of the TCSs of the P–P model raindrops versus the mean raindrop radius (a) at a frequency of 21.225 GHz have been obtained and shown in Fig. 4. The refractive index of water computed at this frequency and at a temperature of 20° using Ray's Fortran program [31] is given by $n_r = (6.4632 - i2.8101)$. The TCSs of the P–P model raindrops obtained at this frequency by Li *et al.* [5], [6] using the boundary-perturbation and point-*matching* techniques are compared with those calculated in this paper using the *simple* method. Comparison shows only slight differences. It is found that an intersection exists between the two curves. Careful checking shows that the intersection comes from the computed effective radii of the P–P raindrop model (see Table I). When the raindrop size becomes very large, in fact, the small perturbation approximation used in [5] is no longer so accurate that a slight over-estimation of TCSs is encountered. This technique based on the effective radii of the scatterers achieves better accuracy than that in [5].

V. Specific Attenuation: Prediction and Experiment

To further examine the applicability of the method developed and the results obtained, the predicted specific microwave attenuation is compared with those measured data collected in Singapore at a frequency of 21.225 GHz over a line-of-sight distance of 1.1 km with a slant angle of about 5° (see [32] for the regressed or best fit curves). The system setup for data collection and the techniques for data integration have been detailed in [33] where both specific rainfall attenuation and rainrates were obtained. Additional information about the specific attenuation can be found from the literature [34].

The specific attenuation $\mathcal{A}$ (in dB/km) of microwaves due to rainfall can be computed numerically using the following integration:

$$\mathcal{A} = 4.343 \times 10^3 \int_0^{a_{\max}} Q_T(\overline{a}) \cdot N(\overline{a})\, d\overline{a}, \quad \text{[in dB/km]} \tag{18}$$

where $Q_T(\overline{a})$ denotes the TCS' (17), and $N(\overline{a})$ represents the distribution of raindrop sizes. To numerically integrate the specific attenuation, a continuous variation of the TCS argument $a_{\text{eff}} = \overline{a}/\sqrt{1-\nu}$ may increase the computational speed. A least squares fit curve has been obtained and expressed by the following formula:

$$a_{\text{eff}}|_{\text{spheroid}} = 1.061\,553\overline{a} - 0.017\,913\,12\overline{a}^2 + 0.007\,348\,77\overline{a}^3$$
$$a_{\text{eff}}|_{\text{P–P model}} = 1.111\,582\overline{a}.$$

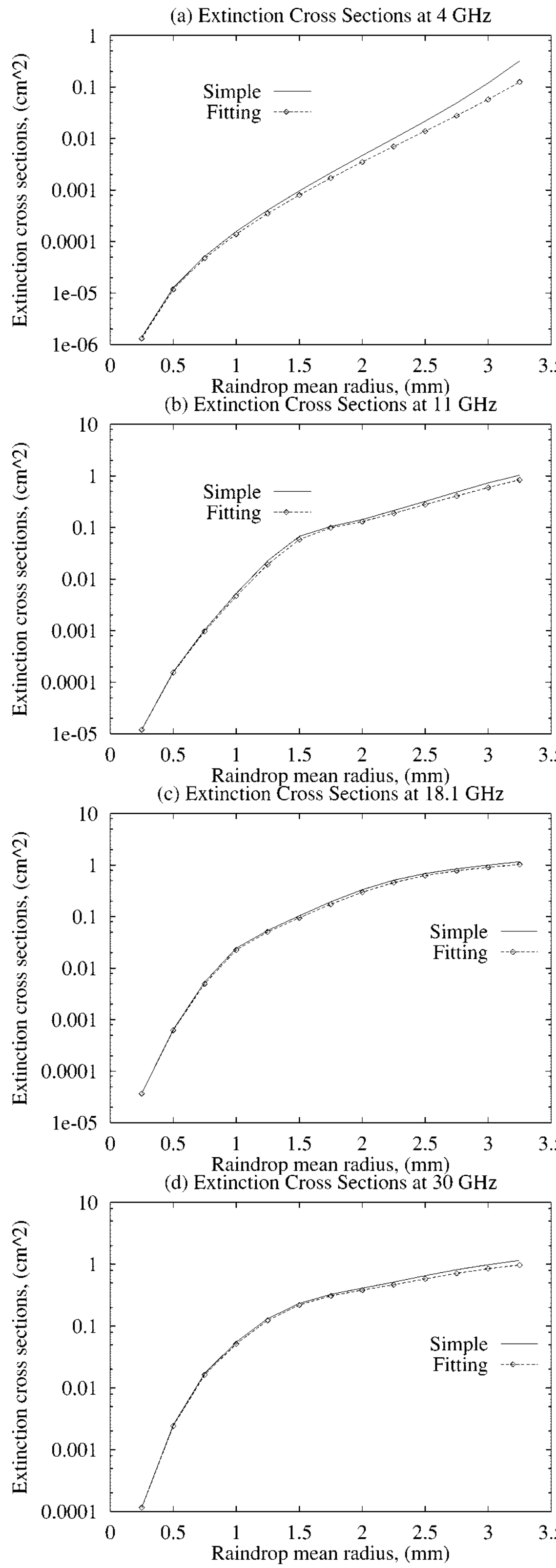

Fig. 3. TCSs (in centimeters^2) of spheroidal raindrops numerically computed at frequencies of 4, 11, 18.1, and 30 GHz and at temperature of 20 °C.

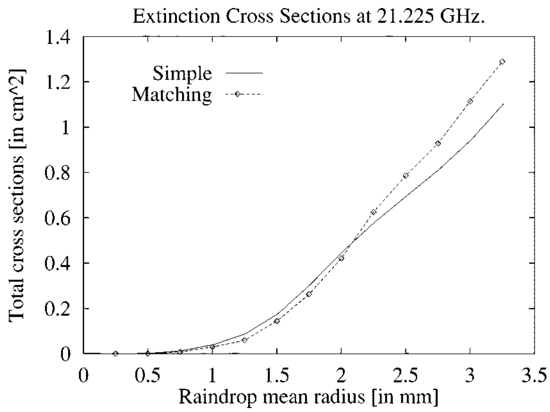

Fig. 4. TCSs of the P–P model raindrops versus the mean radius at a frequency of 21.225 GHz.

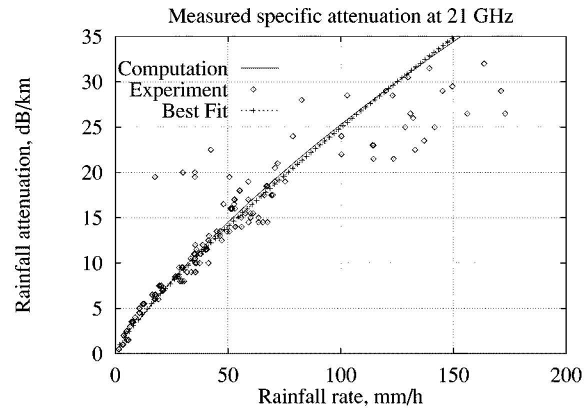

Fig. 5. Comparison of specific rainfall attenuation of horizontally polarized microwaves at 21.225 GHz.

The raindrop size distribution for the Singapore's tropical environment was obtained earlier by Yeo *et al.* [33] and revised later by Li *et al.* [35]. The new raindrop size distribution can be expressed as follows:

$$N(\overline{a}) = 0.031\,783\,2 \exp\left[-2.72R^{-0.197\,75}D\right] \ (\mathrm{cm}^{-4}) \quad (19)$$

where $D = 2\overline{a}$ is the diameter of a raindrop in millimeters.

Using (18) and (19), we have numerically calculated the specific rainfall attenuation at 21.225 GHz in Fig. 5 where *computation* denotes the predicted results numerically calculated in this paper, *experiment* represents the measured data experimentally collected in Singapore, and *best fit* stands for the best fit curve of the experimental data using the least squares fitting. From Fig. 5, reasonably good agreement between the predicted specific rainfall attenuation and the measured data (or the best fit curve) is obtained at 21.225 GHz.

VI. Conclusion and Discussion

Based on the dyadic Green's function technique and the scattering-radiation conversion, an efficient and simple method is developed in this paper to investigate the plane wave scattering due to raindrops. Instead of solving the boundary-value problem or integrating the approximate transmitted field inside the scatterers, the scattered electromagnetic fields are obtained by means of integrating the volumetric current distribution of a source at infinity and the scattering dyadic Green's function.

Using the existing scattering Green's function [25], [36] and the Mie scattered fields expanded in terms of a series of spherical vector wave functions, we have derived the current distribution of an assumed source located at infinity. This source generates the plane waves with horizontal and vertical polarizations. Consequently, the scattered field due the scatterer's surface have been integrated straightforwardly from the current density obtained and the scattering dyadic Green's function derived. The TCSs and the specific attenuation due to the spheroidal raindrops and the P–P model raindrops are numerically computed. To examine the applicability of the method developed and results obtained, the numerical TCSs of the spheroidal raindrops are compared with Morrison and Cross's results [8], those of the P–P model raindrops with Li *et al.* [6], and the specific microwave attenuation due to spheroidal raindrops with the experimental rainfall microwave attenuation collected in Singapore at 21.225 GHz.

The merit of the approximation developed in this paper can be seen from the following aspects. First, this method provides a technique to convert the scattering problem to a specific radiation problem so that the existing theory for the radiation problems can be directly used to the scattering problem. Such a technique successfully employed here can also be used in some other scattering problems. Second, this method that uses spherical vector wave functional expansion together with the dyadic Green's technique, makes the derivation of the approximate scattered field much compact and straightforward. As can be seen from (17), the TCSs can be represented in a very simple form. Third, with the small perturbation expansion and the equivalent radius of the scatterer, this method is simple and efficient for analyzing raindrop scatterers of slightly distorted shapes.

The applicability of this technique has been demonstrated in Figs. 3–5, respectively, where close agreements are obtained between the TCSs of spheroidal raindrops computed using the method presented in this paper and by Morrison and Cross [8] using the least squares process of the boundary conditions, between the TCSs of the P–P model raindrops so obtained and by Li *et al.* [5] using the boundary-perturbation and point-matching techniques and between the specific rainfall attenuation predicted using spheroidal raindrops and data collected in Singapore.

While the Mie scattering theory together with the existing local distribution of raindrop sizes [35] can predict the specific rainfall attenuation for vertical polarization well [6], the simple approach given in this paper may, as a supplement, efficiently predict the specific rainfall attenuation for horizontal polarization. The local distribution of raindrop sizes of [35] was generated applying the Mie scattering theory and utilizing the least squares process of the experimental data at 21.225 GHz for vertical polarization. While the specific attenuation for vertical polarization can be predicted using spherical model and the local distribution of raindrop sizes (DSD), modification from the spherical to spheroidal raindrops must be made when the attenuation under horizontal polarization is to be accurately predicted.

APPENDIX I
UNBOUNDED AND SCATTERING DYADIC GREEN'S FUNCTIONS

The dyadic Green's function involved in the integration (2) was sometimes assumed to be the one in `free`-space for mathematical simplicity. In fact, it is not true. It should be the electric type of dyadic Green's function `outside` the arbitrarily shaped scatterer, $\overline{\boldsymbol{G}}_e(\boldsymbol{r}, \boldsymbol{r}')$. According to the principle of scattering superposition, this dyadic function used in integral (2) consists of the *unbounded* dyadic Green's function and the *scattering* dyadic Green's function, i.e.,

$$\overline{\boldsymbol{G}}_e = \overline{\boldsymbol{G}}_{e0} + \overline{\boldsymbol{G}}_{es}. \tag{A.1}$$

The unbounded Green dyadic $\overline{\boldsymbol{G}}_{e0}$ for $r \gtrless r'$ is given [25] by

$$\overline{\boldsymbol{G}}_{e0}(\boldsymbol{r}, \boldsymbol{r}') = -\frac{ik_0}{4\pi}\sum_{n=1}^{\infty}\sum_{m=0}^{n}(2-\delta_0)\frac{2n+1}{n(n+1)}\frac{(n-m)!}{(n+m)!} \cdot \begin{cases} \boldsymbol{M}^{(2)}_{\substack{e\\o}mn}(k_0)\boldsymbol{M}'_{\substack{e\\o}mn}(k_0) + \boldsymbol{N}^{(2)}_{\substack{e\\o}mn}(k_0)\boldsymbol{N}'_{\substack{e\\o}mn}(k_0) \\ \boldsymbol{M}_{\substack{e\\o}mn}(k_0)\boldsymbol{M}'^{(2)}_{\substack{e\\o}mn}(k_0) + \boldsymbol{N}_{\substack{e\\o}mn}(k_0)\boldsymbol{N}'^{(2)}_{\substack{e\\o}mn}(k_0) \end{cases} \tag{A.2a}$$

while the scattering Green dyadic $\overline{\boldsymbol{G}}_{es}$ outside an effective sphere is given [36] by

$$\overline{\boldsymbol{G}}_{es}(\boldsymbol{r}, \boldsymbol{r}') = -\frac{ik_0}{4\pi}\sum_{n=1}^{\infty}\sum_{m=0}^{n}(2-\delta_0)\frac{2n+1}{n(n+1)}\frac{(n-m)!}{(n+m)!} \cdot \Big[\mathcal{S}^a_n(a_e)\boldsymbol{M}_{\substack{e\\o}mn}(k_0)\boldsymbol{M}'^{(2)}_{\substack{e\\o}mn}(k_0) + \mathcal{S}^b_n(a_e)\boldsymbol{N}_{\substack{e\\o}mn}(k_0)\boldsymbol{N}'^{(2)}_{\substack{e\\o}mn}(k_0)\Big] \tag{A.2b}$$

where the spherical vector wave functions $\boldsymbol{M}_{\substack{e\\o}mn}$ and $\boldsymbol{N}_{\substack{e\\o}mn}$ in the spherical coordinates system can be expressed by

$$\boldsymbol{M}^{(\bullet)}_{\substack{e\\o}mn}(k) = \mp z^{(\bullet)}_n(kr)\frac{mP^m_n(\cos\theta)}{\sin\theta}\frac{\sin}{\cos}m\phi\hat{\boldsymbol{\theta}} - z^{(\bullet)}_n(kr)\frac{dP^m_n(\cos\theta)}{d\theta}\frac{\cos}{\sin}m\phi\hat{\boldsymbol{\phi}} \tag{A.3a}$$

and

$$\boldsymbol{N}^{(\bullet)}_{\substack{e\\o}mn}(k) = \frac{n(n+1)z^{(\bullet)}_n(kr)}{kr}P^m_n(\cos\theta)\frac{\cos}{\sin}m\phi\hat{\boldsymbol{r}} + \frac{d\left[rz^{(\bullet)}_n(kr)\right]}{kr\,dr}\frac{dP^m_n(\cos\theta)}{d\theta}\frac{\cos}{\sin}m\phi\hat{\boldsymbol{\theta}} \mp \frac{d\left[rz^{(\bullet)}_n(kr)\right]}{kr\,dr}\frac{mP^m_n(\cos\theta)}{\sin\theta}\frac{\sin}{\cos}m\phi\hat{\boldsymbol{\phi}} \tag{A.3b}$$

The symbol $z_n(kr)$ represents the spherical Bessel functions of n-order; $P^m_n(\cos\theta)$ stands for the associated Legendre function; the prime denotes those functions associated with the coordinates system (r', θ', ϕ'); the symbol $^{(2)}$ denotes that the spherical Bessel function included in the vector wave functions takes the spherical Hankel functions of the second kind [i.e., the spherical Bessel functions of the fourth kind ($z^{(4)}_n(kr) = h^{(2)}_n(kr)$)]; and δ^n_m (=1 for $m = n$; and zero for $m \neq n$) denotes the Kronecker symbol.

The scattering coefficients $\mathcal{S}^a_n(a_e)$ and $\mathcal{S}^b_n(a_e)$ of the dyadics in (A.2b) can be solved from the equation system (11)–(14) given in the old edition of Tai's book [25, p. 183, 1st ed.]. They can be also found directly from the reduced form of the generalized formulation of the scattering Green dyadic's coefficients presented recently by Li *et al.* [36]. The expressions are

$$\mathcal{S}^a_n(a_e) = \frac{-j_n(\zeta\rho)[\rho j_n(\rho)]' + j_n(\rho)[\zeta\rho j_n(\zeta\rho)]'}{j_n(\zeta\rho)[\rho h^{(2)}_n(\rho)]' - h^{(2)}_n(\rho)[\zeta\rho j_n(\zeta\rho)]'}, \tag{A.4a}$$

$$\mathcal{S}^b_n(a_e) = \frac{-j_n(\rho)[\zeta\rho j_n(\zeta\rho)]' + \zeta^2 j_n(\zeta\rho)[\rho j_n(\rho)]'}{h^{(2)}_n(\rho)[\zeta\rho j_n(\zeta\rho)]' - \zeta^2 j_n(\zeta\rho)[\rho h^{(2)}_n(\rho)]'} \tag{A.4b}$$

where $\zeta = \sqrt{\epsilon_r}$ is the relative refractive index given numerically by Ray [31] in his Fortran program, and ρ is the intermediate defined by the product of the propagation constant and the effective radius of the scatterer, i.e., $k_0 a_e$.

APPENDIX II
VOLUMETRIC CURRENT DISTRIBUTION

In electromagnetic wave theory, there are two well-known areas: 1) the radiation due to an antenna located in an environment where scatterers of different geometries are present and 2) the scattering of a plane wave by scatterers of different geometries. The radiation due to an antenna in a structure is regarded as an active problem while the scattering of the plane wave by such a structure may be considered as a passive problem. Usually, the methods utilized in the two areas for calculating the fields in the regions separated by the scatterers are not exactly the same.

This section aims at relating the scattering problem to the radiation problem and deriving the volumetric current distribution of an electric source that is located at infinity and generates the plane wave. Thus, the scattering problems can be considered as the specific radiation problems where the radiated source is located at infinity. Furthermore, the electromagnetic fields in the regions separated by the scatterers can be easily formulated using the methods already developed for the radiation problems.

To derive such a distribution, the coordinate translation shown in Fig. 6 should be employed here. In this figure, the fields are observed in the coordinates system (r, θ, ϕ) and the point source at the infinity is located in the coordinates system (r'', θ'', ϕ''); $\boldsymbol{r}_0$ denotes the position of the point source with the distance $r_0 \to \infty$, at the polar angle $\theta = \alpha$, and the azimuth angle $\phi = 0$ (the raindrop is symmetrical with respect to the z-axis so that a simple azimuth angle can be chosen); $\boldsymbol{r}'$ represents the position of the differential element in the source region. It can be seen from this figure that the position of the point-source $\boldsymbol{r}_0$ in the field coordinates, the position of a differential element $\boldsymbol{r}'$ in the field coordinates, and the position of the differential element $\boldsymbol{r}''$ in the source coordinates are related by

$$\boldsymbol{r}' = \boldsymbol{r}_0 + \boldsymbol{r}''. \tag{B.1}$$

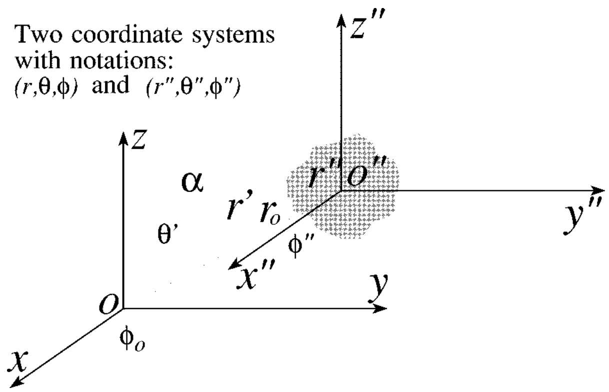

Fig. 6. Coordinate translation.

The source at infinity can be regarded as a point source, therefore a delta function can be used to describe the source. For different polarizations, the source can be expressed by

$$^{I}\boldsymbol{J}(\boldsymbol{r}') = E_I f(r_0)\delta(\boldsymbol{r}' - \boldsymbol{r}_0)\hat{\boldsymbol{\theta}}, \quad \text{(B.2a)}$$
$$^{II}\boldsymbol{J}(\boldsymbol{r}') = E_{II} f(r_0)\delta(\boldsymbol{r}' - \boldsymbol{r}_0)\hat{\boldsymbol{\phi}} \quad \text{(B.2b)}$$

where $f(r_0)$ to be determined is a function of the distance of the point source. The plane waves can be considered as the one excited by the point source that is located at infinity ($r_0 \to \infty$). Since $\boldsymbol{r}_0$ is a constant vector, the vectors $\boldsymbol{r}'$ and $\boldsymbol{r}''$ and their derivatives in the two coordinates systems are related by

$$d\boldsymbol{r}' = d\boldsymbol{r}'' \quad \text{(B.3a)}$$
$$\boldsymbol{r}' - \boldsymbol{r}_0 = \boldsymbol{r}'' \quad \text{(B.3b)}$$

so that (B.2) can be rewritten as

$$\begin{aligned} ^{I}\boldsymbol{J}(\boldsymbol{r}') &= E_I f(r_0)\delta(\boldsymbol{r}'')\hat{\boldsymbol{\theta}} \\ &= E_I f(r_0)\frac{\delta(r''-0)\delta(\theta''-0)\delta(\phi''-0)}{[r'']^2 \sin\theta''}\hat{\boldsymbol{\theta}} \quad \text{(B.4a)} \\ ^{II}\boldsymbol{J}(\boldsymbol{r}') &= E_{II} f(r_0)\delta(\boldsymbol{r}'')\hat{\boldsymbol{\phi}} \\ &= E_{II} f(r_0)\frac{\delta(r''-0)\delta(\theta''-0)\delta(\phi''-0)}{[r'']^2 \sin\theta''}\hat{\boldsymbol{\phi}}. \quad \text{(B.4b)} \end{aligned}$$

Furthermore, we have

$$\begin{bmatrix} ^{I}\boldsymbol{J}(\boldsymbol{r}') \\ ^{II}\boldsymbol{J}(\boldsymbol{r}') \end{bmatrix} d\boldsymbol{r}' = f(r_0)\begin{bmatrix} E_I\hat{\boldsymbol{\theta}} \\ E_{II}\hat{\boldsymbol{\phi}} \end{bmatrix}\delta(r'')\delta(\theta'')\delta(\phi'')\,dr''\,d\theta''\,d\phi''. \quad \text{(B.5)}$$

Substituting (B.5) into the first integral of (3), we may determine the function $f(r_0)$. Either the dyadic $\boldsymbol{MM}'$ or $\boldsymbol{NN}'$ can be used in the derivation. For simplicity, we choose the dyadic $\boldsymbol{MM}'$ and define the following intermediates

$$\begin{bmatrix} \mathcal{I}_M^I \\ \mathcal{I}_M^{II} \end{bmatrix} = \iiint_V \boldsymbol{M}'_{\substack{e\\o}mn}(k_0)\cdot\begin{bmatrix} ^{I}\boldsymbol{J}(\boldsymbol{r}') \\ ^{II}\boldsymbol{J}(\boldsymbol{r}') \end{bmatrix} d\boldsymbol{r}'. \quad \text{(B.6)}$$

Substitution of (B.5) into (B.6) leads to $r' \to r_0$, $\theta' \to \alpha$, and $\phi' \to 0$ in the integral containing the vector eigenfunction $\boldsymbol{M}'_{\substack{e\\o}mn}$. Thus, we finally obtain the following expressions:

$$\begin{bmatrix} \mathcal{I}_M^I \\ \mathcal{I}_M^{II} \end{bmatrix} = \pm\begin{bmatrix} E_I \\ E_{II} \end{bmatrix} f(r_0)h_n^{(2)}(k_0r_0)\begin{bmatrix} \dfrac{mP_n^m(\cos\alpha)}{\sin\alpha} \\ \dfrac{dP_n^m(\cos\alpha)}{d\alpha} \end{bmatrix}. \quad \text{(B.7)}$$

(B.7) may be further reduced using the asymptotic form of Hankel function for large argument given as follows:

$$h_n^{(2)}(k_0r_0) = i^{n+1}\frac{e^{-ik_0r_0}}{k_0r_0} \quad \text{(B.8a)}$$
$$\frac{d\left[(k_0r_0)h_n^{(2)}(k_0r_0)\right]}{(k_0r_0)\,d(k_0r_0)} = i^n\frac{e^{-ik_0r_0}}{k_0r_0}. \quad \text{(B.8b)}$$

Since the first term of (3) can be expressed by (4a) together with (5), substituting (B.7) together with (B.8a) into (3), we have

$$\lim_{r_0\to\infty}\left[-\frac{ik_0\omega\mu_0}{4\pi}f(r_0)\frac{e^{-ikr_0}}{k_0r_0}\right] = 1. \quad \text{(B.9)}$$

Thus, the unknown function $f(r_0)$ is determined and given by

$$f(r_0) = \frac{i4\pi}{\omega\mu_0}r_0e^{ik_0r_0}. \quad \text{(B.10)}$$

Substituting (B.10) back to the definition of the current distribution in (B.2) and then substituting (B.2) into (3), we find the coefficient $^{I}_{II}\mathcal{B}_{\substack{e\\o}mn}$ to be the same as that given by (5b). Thus, the current distribution obtained is verified.

If the volumetric current distribution is not a delta function, the simple analysis made here should be modified and the translational addition theorems derived for spherical waves by Stratton [37] and Friedman and Russek [38] and for spherical vector wave functions by Stein [39] and Cruzan [40] must be applied in the rigorous formulation.

REFERENCES

[1] A. F. Stevenson, "Solution of electromagnetic scattering problems as power series in the ratio (dimension of scatterer)/wavelength," *J. Appl. Phys.*, vol. 24, pp. 1134–1142, 1953.
[2] ——, "Electromagnetic scattering by an ellipsoid in the third approximation," *J. Appl. Phys.*, vol. 24, pp. 1143–1151, 1953.
[3] T. Oguchi, "Attenuation of electromagnetic wave due to rain with distorted raindrops," *J. Radio Res. Labs.*, vol. 7, pp. 467–485, 1960.
[4] ——, "Attenuation of electromagnetic wave due to rain with distorted raindrops—Part II," *J. Radio Res. Labs.*, vol. 11, pp. 19–44, 1964.
[5] L. W. Li, P. S. Kooi, M. S. Leong, T. S. Yeo, and M. Z. Gao, "Microwave attenuation by realistically distorted raindrops: Part I—Theory," *IEEE Trans. Antennas Propagat.*, vol. 43, pp. 811–822, Aug. 1995.
[6] ——, "Microwave attenuation by realistically distorted raindrops: Part II—Predictions," *IEEE Trans. Antennas Propagat.*, vol. 43, pp. 823–828, Aug. 1995.
[7] J. A. Morrison and T. S. Chu, "Perturbation calculations of rain-induced differential attenuation and differential phase shift at microwave frequencies," *Bell Syst. Tech. J.*, vol. 52, pp. 1907–1913, 1973.
[8] J. A. Morrison and M. J. Cross, "Scattering of a plane electromagnetic wave by axisymmetric raindrops," *Bell Syst. Tech. J.*, vol. 53, pp. 955–1019, 1974.
[9] P. C. Waterman, "Matrix formulation of electromagnetic scattering," *Proc. IEEE*, vol. 53, pp. 805–812, 1965.

[10] ——, "Scattering by dielectric obstacles," *Alta Freq.*, vol. 38, pp. 348–352, 1969.
[11] P. Barber and C. Yeh, "Scattering of electromagnetic waves by arbitrarily shaped dielectric bodies," *Appl. Opt.*, vol. 14, pp. 2864–2872, 1975.
[12] C. Warner and A. Hizal, "Scattering and depolarization of microwaves by spheroidal raindrops," *Radio Sci.*, vol. 11, pp. 921–930, 1976.
[13] K. K. Mei, "Unimoment method of solving antenna and scattering problems," *IEEE Trans. Antennas Propagat.*, vol. AP-22, pp. 760–766, Nov. 1974.
[14] S.-K. Chang and K. K. Mei, "Application of the unimoment method to electromagnetic scattering of dielectric cylinders," *IEEE Trans. Antennas Propagat.*, vol. AP-24, pp. 35–42, Jan. 1976.
[15] T. Oguchi, "Scattering from hydrometeors: A survey," *Radio Sci.*, vol. 16, pp. 691–730, 1981.
[16] ——, "Electromagnetic wave propagation and scattering in rain and other hydrometeors," *Proc. IEEE*, vol. 71, pp. 1029–1078, Sept. 1983.
[17] R. L. Olsen, D. V. Rogers, and D. B. Hodge, "The aR^b relation in the calculation of rain attenuation," *IEEE Trans. Antennas Propagat.*, vol. AP-26, pp. 318–329, Mar. 1978.
[18] D. M. A. Jones, "The shape of raindrops," *J. Atmos. Sci.*, vol. 16, pp. 504–510, 1959.
[19] H. R. Pruppacher and K. V. Beard, "A wind tunnel investigation of the internal circulation and shape of water drops falling at terminal velocity in air," *Quart. J. R. Met. Soc.*, vol. 96, pp. 247–256, 1970.
[20] L. W. Li, P. S. Kooi, M. S. Leong, and T. S. Yeo, "On the simplified expression of realistic raindrop shapes," *Microwave Opt. Technol. Lett.*, vol. 7, no. 4, pp. 201–205, March 1994.
[21] H. R. Pruppacher and R. L. Pitter, "A semi-empirical determination of the shape of cloud and rain drops," *J. Atmos. Sci.*, vol. 28, pp. 86–94, 1971.
[22] J. O. Laws and D. A. Parsons, "The relation of raindrop-size to intensity," *Trans. Amer. Geophys. Union*, vol. 24, pp. 452–460, 1943.
[23] T. Oguchi, "Scattering properties of Pruppacher-and-Pitter form raindrops and cross polarization due to rain: Calculations at 11, 13, 19.3, and 34.8 GHz," *Radio Sci.*, vol. 12, pp. 41–51, 1977.
[24] W. C. Chew, *Waves and Fields in Inhomogeneous Media*. New York: Van Nostrand Reinhold, 1990.
[25] C. T. Tai, *Dyadic Green's Functions in Electromagnetic Theory*, 2nd ed. Piscataway, NJ: IEEE Press, 1994.
[26] M. Kerker, *The Scattering of Light and Other Electromagnetic Radiation*. New York: Academic, 1969.
[27] K. Shimizu, "Modification of the Rayleigh–Debye approximation," *J. Opt. Soc. Amer. A*, vol. 73, pp. 504–507, 1983.
[28] J. E. Gordon, "Simple method for approximating Mie scattering," *J. Opt. Soc. Amer. A*, vol. 75, pp. 156–159, 1985.
[29] A. R. Holt, N. K. Uzunoglu, and B. G. Evans, "An integral equation solution to the scattering of electromagnetic radiation by dielectric spheroids and ellipsoids," *IEEE Trans. Antennas Propagat.*, vol. AP-26, pp. 706–712, Sept. 1978.
[30] V. A. Erma, "An exact solution for the scattering of electromagnetic waves from conductors of arbitrary shape: I. Case of cylindrical symmetry," *Phys. Rev.*, vol. 173, pp. 1243–1257, 1968.
[31] P. S. Ray, "Broadband complex refractive indices of ice and water," *Appl. Opt.*, vol. 11, pp. 1836–1844, 1972.
[32] T. S. Yeo, P. S. Kooi, and M. S. Leong, "Microwaves attenuation measurement in Singapore," in *Proc. 1994 Asia-Pacific Microwave Conf.*, Tokyo, Japan, Dec. 1994, pp. 193–196.
[33] ——, "A two-year measurement of rainfall attenuation of CW microwaves in Singapore," *IEEE Trans. Antennas Propagat.*, vol. 41, pp. 709–712, June 1993.
[34] T. S. Yeo, P. S. Kooi, M. S. Leong, and S. S. Ng, "Microwave attenuation due to rainfall at 21.225 GHz in the Singapore environment," *Electron. Lett.*, vol. 26, pp. 1021–1022, 1990.
[35] L. W. Li, T. S. Yeo, P. S. Kooi, and M. S. Leong, "Comment on raindrop size distribution model," *IEEE Trans. Antennas Propagat.*, vol. 42, p. 1360, Sept. 1994.
[36] ——, "Electromagnetic dyadic Green's function in spherically multilayered media," *IEEE Trans. Microwave Theory Tech.*, pt. A, vol. 42, pp. 2302–2310, Dec. 1994.
[37] J. A. Stratton, *Electromagnetic Theory*. New York: McGraw-Hill, 1941.
[38] B. Friedman and J. Russek, "Addition theorems for spherical waves," *Quart. Appl. Math.*, vol. 12, pp. 13–23, 1954.
[39] J. Seymour Stein, "Addition theorems for spherical wave functions," *Quart. Appl. Math.*, vol. 19, pp. 15–24, 1961.
[40] O. R. Cruzan, "Translational addition theorems for spherical vector wave functions," *Quart. Appl. Math.*, vol. 20, pp. 33–40, 1962.

Le-Wei Li (S'91–M'92–SM'96) received the B.Sc. degree in physics from Xuzhou Normal University, Xuzhou, China, in 1984, the M.Eng.Sc. degree in electrical engineering from the China Research Institute of Radiowave Propagation (CRIRP), Xinxiang, China, in 1987, and the Ph.D. degree in electrical engineering from Monash University, Melbourne, Australia, in 1992.

In 1992, he was with La Trobe University (jointly with Monash University), Melbourne, Australia, as a Research Fellow. Since 1992, he has been with the Department of Electrical Engineering, National University of Singapore, where he is currently an Associate Professor. His current research interests include electromagnetic theory, radio wave propagation and scattering in various media, microwave propagation and scattering in tropical environment, and analysis and design of various antennas.

Dr. Li was a recipient of the Best Paper Award from the Chinese Institute of Communications for his paper published in *Journal of China Institute of Communications* in 1990, and the Prize Paper Award from the Chinese Institute of Electronics for his paper published in *Chinese Journal of Radio Science* in 1991. He was selected to receive a Ministerial Science and Technology Advancement Award by Ministry of Electronic Industries, China, in 1995 and a National Science and Technology Advancement Award with medal by National Science and Technology Committee, China, in 1996. He has been a member of the Electromagnetics Academy since 1998.

Tat-Soon Yeo (M'80–SM'93) received the B.Eng. (honors) and M.Eng. degrees from the National University of Singapore, in 1979 and 1981, respectively, and the Ph.D. degree from the University of Canterbury, New Zealand, in 1985.

Since 1985, he has been with the Electrical Engineering Department of the National University of Singapore, where he is currently an Associate Professor. His current research interests are in wave propagation and scattering, antennas, and numerical techniques.

Dr. Yeo received the 1997 Defence Science Organization (DSO) Research and Development Award from DSO National Laboratories, Singapore, in 1997. He has served as a Guest Editor for the Special Issue of IEEE TRANSACTIONS GEOSCIENCE AND REMOTE SENSING in 1998 and was on the Editorial Board of IEEE TRANSACTIONS ON MICROWAVE THEORY AND TECHNIQUES since 1997.

Pang-Shyan Kooi (M'75) received the B.Sc. degree in electrical engineering from the National Taiwan University, Taipei, in 1961, the M.Sc. (Tech) degree in electrical engineering from the University of Manchester Institute of Science and Technology (UMIST), Manchester, U.K., in 1963, and the D.Phil. degree in engineering science from Oxford University, U.K., in 1970.

Since 1970, he has been with the Electrical Engineering Department, National University of Singapore, where he is currently a Professor of electrical engineering. His current research interests are microwave and millimeter-wave circuits, antennas, and solid-state microwave sources.

Dr. Kooi is a Fellow of the Institution of Electrical Engineers (IEE), London, U.K.

Mook-Seng Leong (M'81–SM'98) received the B.Sc. degree in electrical engineering (first class honors) and the Ph.D. degree in microwave engineering from the University of London, U.K., in 1968 and 1971, respectively.

He is currently a Professor of electrical engineering at the National University of Singapore. He is a member of the Editorial Board for *Microwave and Optical Technoloogy Letters* and *Wireless Mobile Communications*. His main research interests include antenna and waveguide boundary-value problems.

Dr. Leong is a member of the Massachusetts Institute of Technology (MIT)-based Electromagnetic Academy, Cambridge, MA, and a Fellow of the Institution of Electrical Engineers (IEE), London, U.K. He received the 1996 Defence Science Organization (DSO) Research and Development Award from DSO National Laboratories, Singapore in 1996.